https://doi.org/10.1595/205651324X16965116259515 *Johnson Matthey Technol. Rev.*, 2024, **68**, (1), 102–111

JOHNSON MATTHEY
TECHNOLOGY REVIEW

technology.matthey.com

Rhodium and Rhodium-Alloy Films and Nanoparticles: Part II

A review of new applications for rhodium and its alloys

Yicheng Zhou, Wangping Wu*
Electrochemistry and Corrosion Laboratory, School of Mechanical Engineering and Rail Transit, Changzhou University, Changzhou 213164, China

Qinqin Wang
School of Mechanical Engineering, Yangzhou University, Yangzhou 225127, China

Liangbing Wang
Avic Tianjin Aviation Electro-mechanical Co Ltd, Tianjin 300308, China

***Email:** wwp3.14@163.com; wuwping@cczu.edu.cn

PEER REVIEWED

Received 24th October 2022; Revised 28th February 2023; Accepted 20th March 2023; Online 22nd March 2023

Part I of this review covered the synthesis methods for synthesis of rhodium films and nanoparticles (1). In Part II, we review the literature on the current and potential applications of rhodium and rhodium alloy films and nanoparticles in catalysis, components for the glass, chemical and electronic industries, thermal sensors and anticancer drugs.

1. Potential Applications

Significant progress has been made in the preparation of noble metal nanoparticles (NMNPs) by various wet chemical methods. Among the various NMNPs, rhodium is known for its key role in a variety of catalytic reactions such as carbon monoxide oxidation, nitric oxide reduction, hydrogenation, hydroformylation and electrooxidation. In addition, rhodium is particularly stable under harsh reaction conditions and is used in components for the glass, chemical and electronic industries such as optical mirrors, electrical contact and connectors and thermal sensors because of its high resistance to acid/base etching and heat resistance. Rhodium also finds application in anticancer drugs.

1.1 The First Mirror in the International Thermonuclear Experimental Reactor

Optical and imaging systems require high performance for plasma diagnostics. Most plasma-facing components use metallic mirrors for optical diagnostics. Reflectivity influences the quality and reliability of the performance of mirrors. Due to the different sputtering yields of rhodium, the erosion of rhodium mirrors is estimated to be around 4 μm. However, due to its high reflectivity in the visible wavelength range (N 70–80%), rhodium is an attractive candidate for the first mirrors in the International Thermonuclear Experimental Reactor (ITER). Rai *et al*. studied the properties of rhodium thin film on a molybdenum mirror with a thin niobium interlayer (2). Rhodium thin films were deposited by magnetron sputtering, and their properties (reflectivity, morphology and stability) were investigated. **Figure 1** shows the spectral reflectance of rhodium, copper, molybdenum, stainless steel and a rhodium mirror. At wavelength of 800 nm, the reflectivities of rhodium, molybdenum and tungsten are 82%, 56% and 50%, respectively. The advantage of rhodium is obvious in the visible

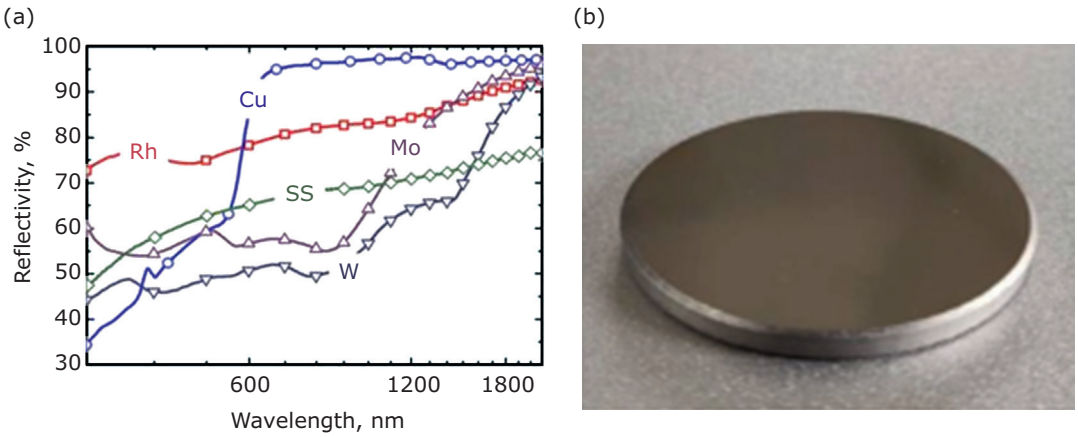

Fig. 1. (a) Spectral reflectance of rhodium, copper, molybdenum, stainless steel. Reprinted from (3) with the permission of AIP Publishing; (b) rhodium mirror deposited by magnetron sputtering (2). Reproduced with permission from SNCSC

wavelength range in comparison to molybdenum or tungsten. As demonstrated in the study of Mostako *et al.*, rhodium thin films exhibited excellent optical properties (4).

1.2 Electronic Applications

Rhodium has stable thermoelectric properties and strong oxidation resistance, which is useful in thermocouples along with platinum (5). Increasing performance of aerospace vehicles requires higher temperatures, faster responses and smaller temperature sensors. In extreme high-temperature environments such as aeroengine turbine blades, combustion chamber walls, high-temperature gas inlets and outlets and hypersonic aircraft surfaces, sensors such as thin-film thermocouples (TFTCs), thin-film strain gauges and thin-film heat flux sensors (6–9) are ideal for transient temperature measurement because of their fast response, small thermal contact and ease of integration. Thin-film sensors have a fast response, small size, easy integration and less interference to monitor the environment (10). Therefore, thin-film sensors have become widely used to measure surface parameters of aeroengine hot components. Oxide semiconductor TFTCs have attracted much attention in engine hot-end components because of their wide temperature measurement range, good oxidation resistance and large Seebeck coefficient (11, 12). However, because the carrier concentration changes with temperature, the repeatability and electromotive force stability of semiconductor TFTCs need to be further improved. Compared with semiconductor TFTCs, noble metal TFTCs have better linearity and repeatability. Through reactive magnetron sputtering, Liu *et al*. prepared a multilayer protective layer composed of Al_2O_3, Si_3N_4 and yttrium-doped SiAlON (YAlO) (see **Figure 2**) (13). The average Seebeck coefficient of TFTCs prepared with the Al_2O_3/Si_3N_4/YAlO protective layer was 10.00 μV °C^{-1} at 1350°C and slightly decreased to 9.90 μV °C^{-1} at 1550°C. The TFTCs appeared to have good stability at high temperature. Meanwhile, the polynomial fitting results also indicated that TFTCs prepared with the Al_2O_3/Si_3N_4/YAlO protective layer had good linearity at high temperature. The drift rate of TFTCs with a Al_2O_3/Si_3N_4/YAlO protective layer was only 2.19 °C h^{-1} at 1350°C and their performance began to decline significantly at 1550°C with a drift rate of 82.89 °C h^{-1}.

Thin-film thermocouples can be used for contact temperature measurement. R-type (platinum-rhodium13-platinum), B-type (platinum-rhodium30-platinum-rhodium6) and S-type (platinum-rhodium10-platinum) thermocouples cannot exceed 1600°C for long-term use but can reach 1800°C for short-term use (14, 15).

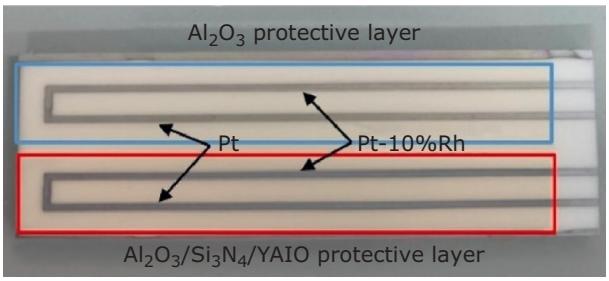

Fig. 2. Photograph of S-type (Pt–Pt10%Rh) TFTCs fabricated on Al_2O_3 substrates. Copyright (2022), reprinted from (13), with permission from Elsevier

Nevertheless, thermocouples easily oxidise in oxidising environments, resulting in excessive temperature measurements. Ultrasonic temperature measurement is a non-contact technique based on the relationship between ultrasonic velocity and measured temperature and the tested temperature can reach 3000°C. Iridium-rhodium alloy ultrasonic guided wave temperature measurement technology has been presented by Wei *et al*. (15). An antioxidation iridium-rhodium alloy sensor was placed directly into a solid rocket motor combustion chamber such that the temperature-sensitive element directly contacted the temperature field and measured the temperature of the combustion chamber.

1.3 Catalytic Applications

Catalysis is very important in chemical engineering. More than 85% of chemical reactions require the participation of catalysts. Among them, chemical reactions involving noble metals account for more than half. Especially for some reactions with high selectivity, directionality, low temperature and low pressure, the participation of noble metals is difficult to replace. At present, rhodium, as an important catalytic material, is widely used in petrochemical, pharmaceutical chemical, fine chemical, environmental protection and other fields. This section outlines research into applications of rhodium catalysts in automotive exhaust, hydroformylation, hydrogenation and electrolysis.

1.3.1 Automotive Exhaust Catalysis

Automobile exhausts have long been a major source of air pollution, especially in big cities. Platinum group elements, for example, platinum, palladium and rhodium, are commonly used to remove nitrogen oxides (NO_x), carbon monoxide and hydrocarbons (HC) from automobile exhausts (17). In recent years, the dramatic increase of the prices of palladium and rhodium have brought about cost pressure for the exhaust gas aftertreatment industry. Traditional noble metal catalysts often suffer from low metal surface dispersion and sintering (18). Therefore, over the past decade, significant efforts have been made to investigate non-noble metals as substitutes for noble metals, very small (sub-nanometre) clusters or even isolated individual atoms for automotive emissions to improve metal efficiency and to mitigate carbon monoxide poisoning.

To reduce costs, the first choice is to reduce the noble metal load. Lan *et al*. (19) obtained an advanced palladium-rhodium catalyst by adjusting the synthesis process based on conventional alumina-loaded palladium and ceria-zirconia (CZ) based oxide loaded rhodium catalysts. A small portion of rhodium is co-impregnated with palladium on alumina, while the other portion remains loaded on CZ. In this way, the co-impregnated rhodium can be used as an additive for the palladium on alumina component. From **Figure 3**, the two catalysts exhibit similar catalytic conversion efficiency of carbon monoxide, HC and nitric oxide, but after hydrothermal aging treatment, the modified catalysts performed better, with higher catalytic conversions over most of the experimental temperature range.

Today, single-atom catalysts (SACs) are attracting increasing research attention in the field of automotive exhaust emission reduction as particle size limitations have been reduced, not only maximizing metal utilisation but also providing many opportunities to modify reaction pathways. The oxide layers of RhO_x are responsible for the high carbon monoxide oxidation activity of rhodium nanoparticles while the inner metallic Rh_0 atoms are inert. The adsorption of CO by rhodium includes the gem-dicarbonyl, linear CO and bridging CO, denoted as $Rh(CO)_2$, Rh(CO) and $Rh_2(CO)$, respectively. Generally, the ratios of $Rh_2(CO)$ and Rh(CO) in all three species increase with increasing particle size. Rhodium catalysts with small particle size consist of higher RhO_x:Rh_0 ratios and therefore have higher specific activity in the carbon monoxide oxidation process. The catalytic performance of rhodium SAC with various carriers for carbon monoxide oxidation was reported by Han *et al*. High activity of ZnO nanowire-loaded rhodium SACs (Rh_1/ZnO-nw) for carbon monoxide oxidation was observed (20). As shown in **Figure 4(a)**, Rh_1/ZnO-nw exhibited the highest carbon monoxide oxidation performance among the three different ZnO-loaded SACs, while Pt_1/ZnO-nw and Au_1/ZnO-nw showed much lower activity.

Rhodium-based catalysts, especially those supported on ceria-based materials, perform well on all points except for catalyst cost, although other heat-resistant supports such as alumina (21) and zirconia (22) have been investigated as catalytically active components. However, the cost of rhodium remains high and is not expected to become lower (23). It is difficult to further reduce the amount of rhodium and increase the activity

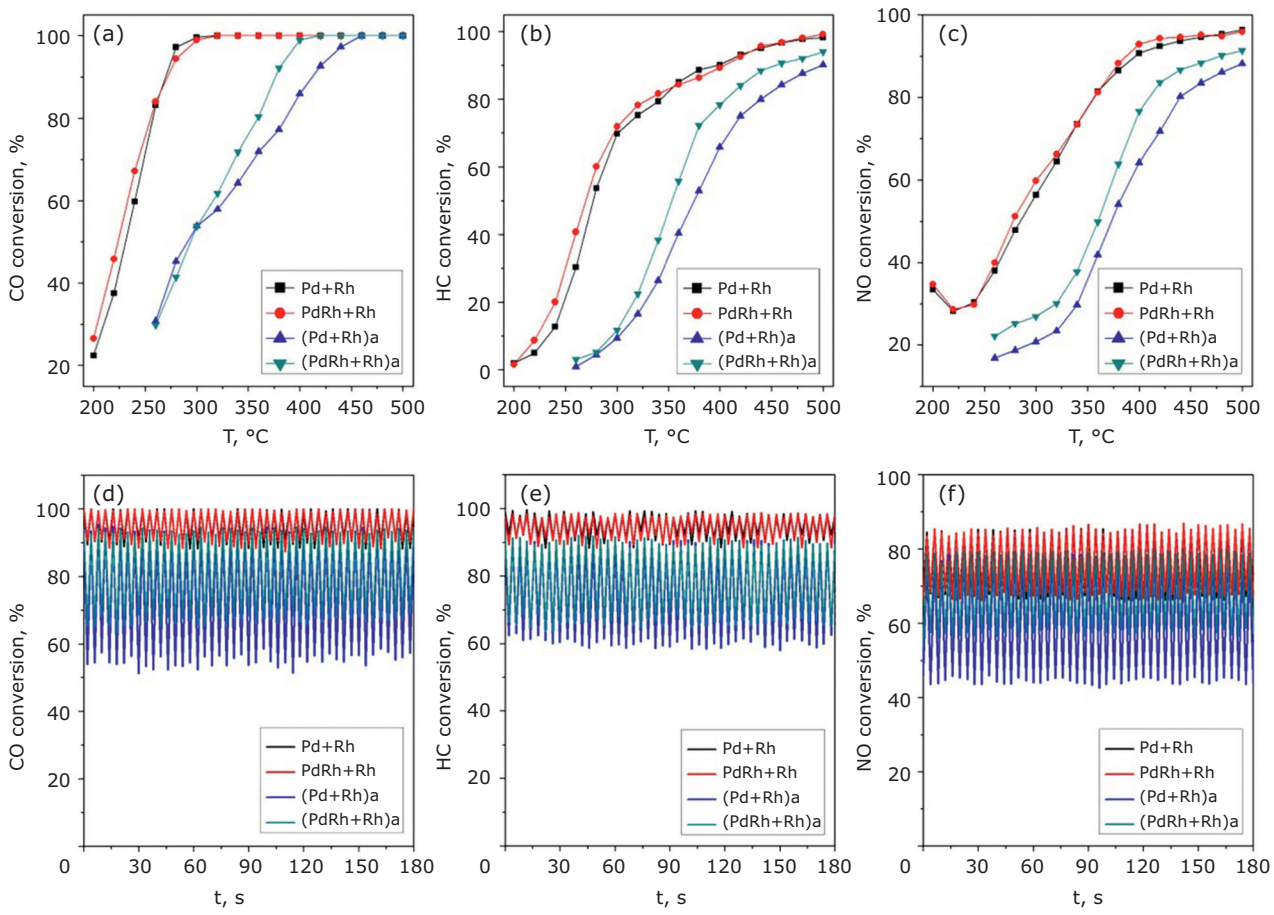

Fig. 3. Catalytic conversion as function of temperature of: (a) CO; (b) HC and (c) NO and as function of time of: (d) CO; (e) HC and (f) NO. Conventional palladium and rhodium catalyst (Pd+Rh), modified palladium-rhodium catalyst (PdRh+Rh). Hydrothermal aged catalysts (Pd+Rh)a and (PdRh+Rh)a, respectively. Reprinted from (19) under Creative Commons Attribution 4.0 License (CC BY-NC-ND 4.0 DEED)

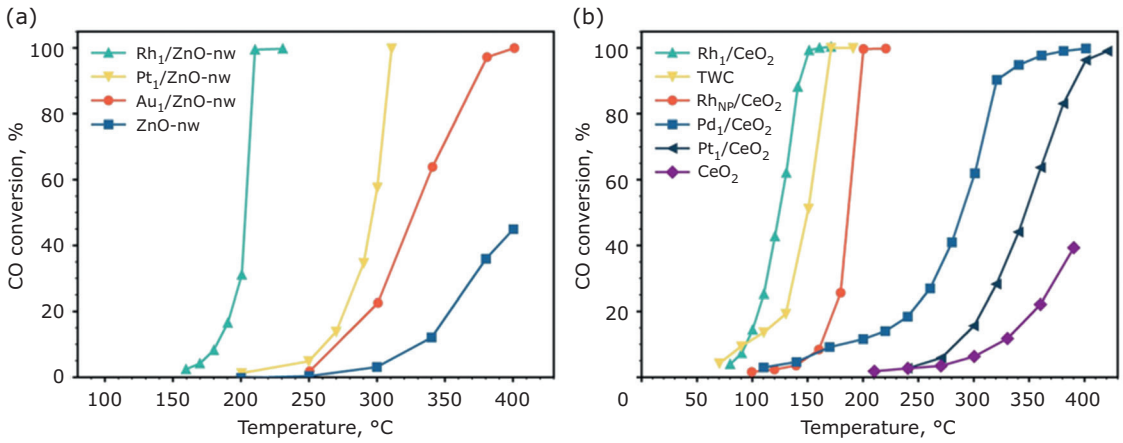

Fig. 4. (a) Catalytic performance of CO oxidation over ZnO-nanowire-supported rhodium, platinum or gold SACs with ZnO nanowire as reference. Measured with 1% CO and 1% O_2 (18). Reproduced with permission from Wiley; (b) catalytic performance of CO oxidation over CeO_2-supported rhodium, palladium or platinum SACs, CeO_2-supported nanoparticle catalysts, commercial TWCs and CeO_2. Measured with 1% CO and 1% O_2. Used with permission of RSC from (20), permission conveyed through Copyright Clearance Center, Inc

of each rhodium. Therefore, some studies have focused on finding alternatives (24) to rhodium-based catalysts.

1.3.2 Hydrogenation Reaction

Catalytic hydrogenation is one of the most important reactions in the pharmaceutical and specialty chemicals industry. It refers to a large group of addition reactions of hydrogen to unsaturated bonds, the simplest addition reactions between hydrogen and the alkenes, alkynes, aldehydes, aromatic nitro compounds and some unsaturated organics in the presence of relevant catalysts (25). As a highly active and chemically stable active component of catalysts, rhodium has always been dominant in hydrogenation reactions. Vlasenko *et al*. (26) fabricated metal-organic framework $Zn_6(mIM)_{12}$ (ZIF-8) loaded with rhodium nanoparticles as a catalyst for hydroformylation. ZIF-8 was obtained as a precipitate by the reaction of $Zn(NO_3)_2{\cdot}6H_2O$ and 2-methylimidazole (HmIM) in methanol at room temperature and then activated by drying under high vacuum at 50°C for 8 h. Catalytically active rhodium nanoparticles were introduced into its pores (**Figure 5**). In the hydroformylation of styrene, both $RhCl_3$@ZIF–8 and Rh@ZIF–8 exhibited excellent catalytic activity.

García *et al*. reported a simple polyol method that utilised ethylene glycol as both reducing agent and reaction medium, in addition to secondary reductants and excess poly(*N*-vinylpyrrolidone) as a stabilising agent (27). In a typical synthesis, precursor solutions of $RhCl_3$ and either $HAuCl_4$ or $AgNO_3$ were simultaneously injected into preheated solvent. The rate of addition was carefully controlled by means of syringe pumps that optimise NP nucleation and growth phases. Well-defined heterometallic nanostructures are of particular interest because synergistic effects between metal atoms of different elements can result in enhancement of the catalytic properties by tuning the average binding energy of the NPs surface. Multimetallic NPs also provide a convenient means to reduce the total amount of the rarest and the most expensive metal *via* dilution with readily available and potentially catalytically inactive metals (27–29).

1.3.3 Hydrogen and Oxygen Evolution Reaction

Hydrogen, with the advantages of high energy storage, no carbon emissions and a byproduct of water, is recognised as a most promising substitute for fossil fuel (30). Electrolysis of water is a renewable and secure way to create hydrogen (31–33). However, the water electrolysis system consumes a large amount of electrical energy because of the large overpotential of the hydrogen evolution reaction (HER). The issue of electrode materials with high electrocatalytic activity and stability is therefore urgent. Noble metals (rhodium, ruthenium, platinum and iridium) have shown remarkable hydrogen production efficiency (34–36). Rhodium is one of the most extensively investigated catalysts for hydrogen generation by hydrolysis owing to its intrinsic catalytic performance toward the reaction (37–40). Liu *et al*. introduced rhodium NPs to $MoSe_2$ nanosheets by deposition. The Rh-$MoSe_2$ nanocomposite achieved electron transfer by tuning the electronic structure of active sites and boosted the HER performance of $MoSe_2$, by combination with rhodium (32). The Rh-$MoSe_2$ nanocomposite presented great enhancement with an extremely low onset potential of 3 mV and overpotential of 31 mV at 10 mA cm^{-2} with long-term stability close to commercial 20 wt% Pt/C. In addition to alloy NPs, heteroatom doping (such as nitrogen, boron, sulfur and phosphorus) is another effective means of improving catalytic performance. The increase of catalytic activity is attributed to the formation of charged sites originating from the different electronegativity values between heteroatom dopants.

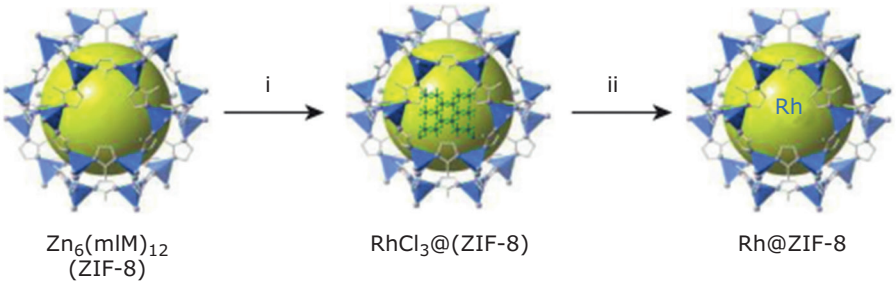

Fig. 5. Composite schematic diagram. Reagents and conditions: i: $RhCl_3$, DMF, room temperature; ii: $NaBH_4$, H_2O, room temperature. Reprinted from (26), with permission from Elsevier

Shen *et al*. designed a multifunctional noble metal/fluorine-doped graphene electrocatalyst using silicon nanowires (Si NWs) as a sacrificial template (35). With a mild solution method, fluorine-doped graphene modified with uniform rhodium nanoparticles (Rh/F-graphene) was obtained. For HER, it exhibited low overpotential of 46 mV (*vs.* reversible hydrogen electrode) @ −10 mA cm^{-2} and small Tafel slope of 30 mV dec^{-1} in 0.5 M H_2SO_4 solutions. In addition, the Turnover frequency value was <0.502 H_2 Rh^{-1} s^{-1} (at 46 mV), larger than that of the 20 wt% Pt/C (0.447 H_2 Pt^{-1} s^{-1}); and the mass activity of Rh/F-graphene-2 was also larger than Pt/C, indicating excellent HER performance (see **Figure 6**). Kim *et al*. also reported rhodium and rhodium-phosphorus catalysts on a carbon paper (CP) substrate *via* electrodeposition and studied the effect of phosphorus atomic surface content on Tafel slopes of Rh-P/CP-# catalysts (33). The Rh-P10/CP-# catalysts demonstrated HER intrinsic activity greater than that of the Rh#/CP and Pt/CP catalysts. Furthermore, the mass activity of Rh#/CP and Rh–P10/CP-# catalysts also surpassed that of Pt/CP catalysts, indicating their potential as alternatives to commercial platinum cathodes in proton exchange membrane water electrolysers (PEMWEs).

Guo *et al*. reported a rational synthetic strategy toward the preparation of sub-10 nm rhodium-iridium nanoparticles as highly efficient oxygen evolution reaction (OER) catalysts under acidic conditions by a modified polyol method (see **Figure 7**) (34). Most significantly, a smaller binding energy gap of O and OOH intermediates was obtained through alloying 22% rhodium into iridium, which resulted in a significant enhancement of OER performance, reflected by a 48 mV decrease in the overpotential to reach a 10 mA cm^{-2} current density and a mass activity that was three times higher than a comparable iridium NP catalyst. Wu *et al*. reported loaded Rh_2P NPs on macroscopic conductive supports with the assistance of binders such as Nafion for water electrolysis on an nitrogen/phoshorus-doped three-dimensional carbon cloth substrate (denoted as Rh_2P–N/P–CC) for highly efficient HER/OER electrocatalysis (36). Rh_2P–N/P–CC outperformed benchmark Pt/C catalysts at only 7.85% equivalent of platinum for HER electrocatalysis and surpassed the RuO_2 catalyst in terms of OER performance in alkaline solution. As a bifunctional electrocatalyst, Rh_2P-N/P-CC enabled stable overall water splitting at current density of 200 mA cm^{-1} under an electrolytic voltage of 1.7 V in alkaline solution. Noble metals have an irreplaceable position in the field of catalysts and

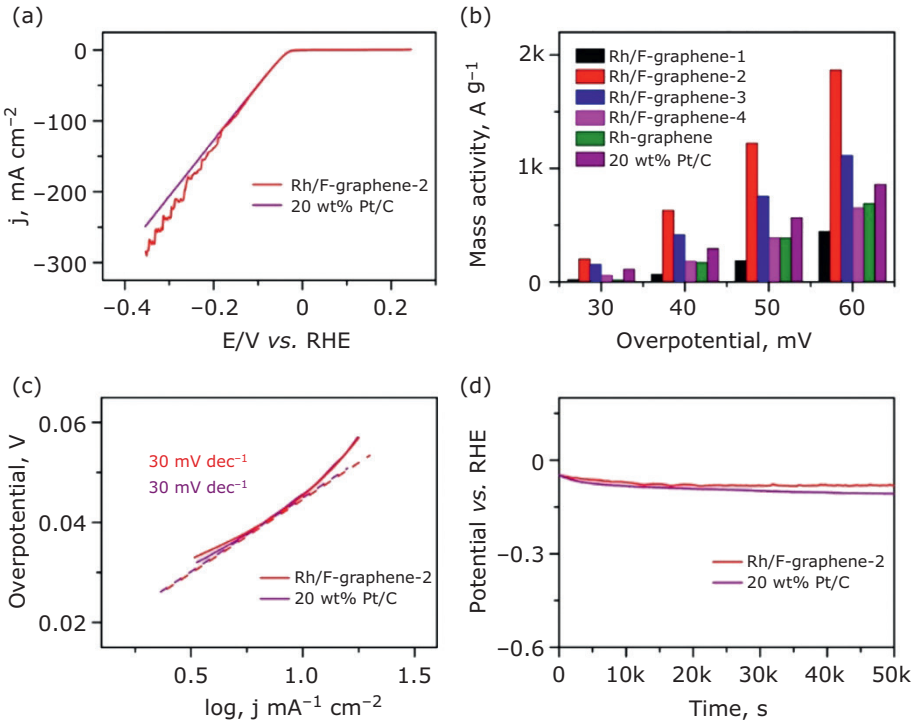

Fig. 6. (a) Polarisation curves of Rh/F-graphene-2 and 20 wt% Pt/C catalysts in oxygen-free 0.5 M H_2SO_4; (b) mass activities of pure metal for 20 wt% Pt/C, different Rh/F-graphene and Rh/graphene catalysts at different overpotentials; (c) corresponding Tafel plots of 20 wt% Pt/C and Rh/F-graphene-2 catalysts derived from (a); and (d) the stability of 20 wt% Pt/C and Rh/F-graphene-2 catalysts by the chronopotentiometry technique @ −10 mA cm^{-2} (32)

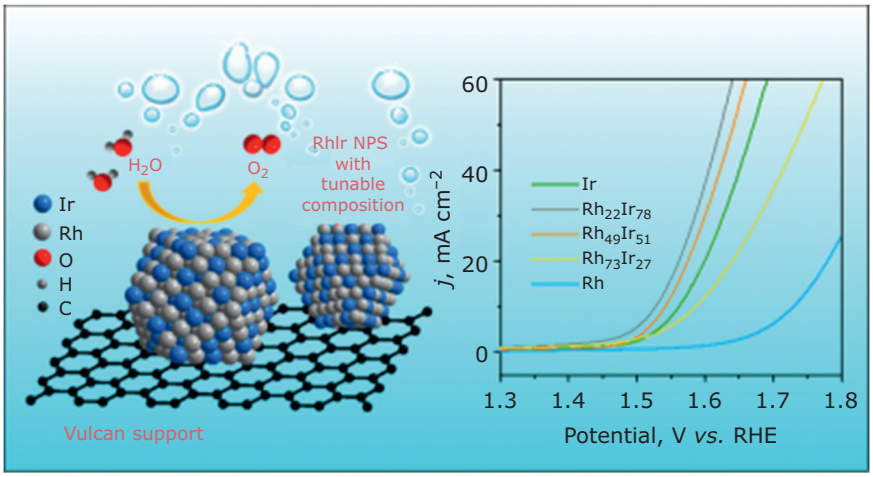

Fig. 7. OER activities on rhodium-idirium nanocatalyst. Reprinted with permission from (34). Copyright (2019) American Chemical Society

Table I Comparison of Hydrogen and Oxygen Evolution Reaction Performance for Electrocatalysts

Catalyst	Electrode	Loading, mg cm^{-2}	Onset potential, mV	Overpotential at 10 mA cm^{-2}, mV	Tafel slope, mV dec^{-1}	Reference
$MoSe_2$	GCE[a]	0.285	67	223	85	(32)
$MoSe_2$/CF	Carbon cloth	–	70	182	69	(42)
1T-$MoSe_2$	GCE	0.14	–	152	52	(43)
B-$MoSe_2$/CC	Carbon cloth	–	–	84	39	(44)
P(Ni,Fe)O_xH_y	Nickel foam	–	–	221	25.1	(45)
$MoSe_2$/rGO	GCE	0.285	125	195	67	(46)
$MoSe_2$/CC	Carbon cloth	–	35	50	38	(47)
Co, Ni-MoS_3	GCE	–	112	171	56.9	(48)
Co-$MoSe_2$	GCE	0.57	–	305	95.2	(49)

[a]Glassy carbon electrode (GCE)

rhodium is no exception. Recently, researchers have investigated electrocatalysts with excellent catalytic performance by controlling the size, shape and structure of NPs (**Table I**).

2. Discussion

Over several years, magnetron sputtering technology has evolved to increase metal ionisation, improve target utilisation, avoid target poisoning in reactive sputtering, increase deposition rates and increase the demand driven by the need to improve sputtering source (cathode target) utilisation, improve the uniformity of deposited films, minimise electrical instabilities such as arcing, achieve directional deposition of metals, allow control of the energy of the ions bombarding the substrate from the film-forming material and reduce operating costs. There are still some important issues to be understood regarding the operation of magnetron sputtering discharges. These include improving the understanding of energy transfer to electrons, observing various instabilities such as spokes and breathing patterns, working gas recovery and self-sputtering recovery.

Pulsed laser deposition (PLD) technology has been widely used in research and industry. However, PLD still cannot fully meet the requirements of thin film technology development and preparation due to three problems. There are difficulties in preparing large-area uniform films, in controlling the deposition rate repeatability and in obtaining smooth films. This is because:

(a) the laser-excited plasma follows the $\cos^n$-α law in spatial angle distribution, where α is the angle between the target normal and the plasma plume and the typical value of the index

n is between seven and 20. It is this directional plasma expansion that makes it difficult to obtain large-area uniform films. At present, this problem can be alleviated to some extent by special laser scanning technology and films with a diameter of 150 mm or even 200 mm and good uniformity can be obtained

(b) as the target surface gradually changes from a smooth surface to a rough surface under the action of laser irradiation, the direction of the excited plasma changes due to the irregular structure of the target surface. This phenomenon makes it difficult to accurately control the repeatability of the deposition rate, thus affecting the prediction of the deposited film thickness

(c) the transient action of laser light with matter produces not only atoms, electrons and ions, but also electrically neutral particles, the size of which ranges from 0.1 μm to 10 μm. Particles embedded inside the film or remaining on the surface can lead to the formation of rough films, making it difficult to obtain smooth films. For special applications such as chemical catalysis, sensing and medical placeholders, such rough surfaces are often required to achieve device performance. However, for most applications, the presence of particles can degrade the optical, mechanical, electrical and magnetic properties of the films, especially for multilayer dielectric and optical films, where particles can cause severe optical scattering and degrade the expected optical performance of the films, so the elimination of these particle is a critical issue to be addressed in PLD.

The electrochemical deposition method is a simple and convenient process, the purity of rhodium obtained is high and the size and morphology of NPs can be controlled by adjusting the magnitude of current and voltage. However, there is still a need to continue to combine knowledge from various fields to solve many problems such as large particle size, easy agglomeration and uncontrollable loading of NPs. It is also necessary to analyse how various factors in the deposition process affect NPs so that the desired morphology can be obtained better and faster.

3. Future Outlook

Rhodium thin films and nanoparticles have an important impact on production, life and scientific research. There are still many challenges in the field of rhodium research. Future research challenges for efficient utilisation of rhodium may include the following points:

(a) To develop facile fabrication methods to precisely control the size and shape of rhodium nanofilms and NPs. The controllable preparation of rhodium NPs relative to other platinum group metals such as gold, silver, palladium and platinum has been extensively studied, but their regulation and application are still limited by size and shape control. Therefore, there is a need to develop new synthetic methods combined with existing control strategies to obtain rhodium NPs with good size and shape control

(b) To explore detailed characterisation and mechanisms. Further enhancement of theoretical simulations and *in situ* characterisation can reveal the synthesis mechanisms and interactions between compounds which can guide the efficient synthesis of high-quality metal nanomaterials

(c) To reduce the amount of noble metals such as rhodium required to obtain benefits. On one hand, alternative noble metal catalysts can be found. On the other hand, noble metals can be loaded onto substrates to improve their catalytic performance per unit. These findings are also applicable to rhodium NPs. The goal is to apply more efficient catalysts to practical applications.

(d) In addition to improving utilisation through nanofilms and NPs, rhodium recycling is essential as it is a non-renewable resource. Most rhodium scrap comes from automotive exhaust catalysts, but it is also very common in petroleum industry catalysts, glass fibre scrap and paint waste liquid. At present, the main recovery methods of rhodium from waste noble metal catalysts are wet recovery and pyrolysis recovery. The development of efficient recovery approaches can also reduce the loss of rhodium.

4. Conclusion

In this review, we aimed to focus on synthesis methods for rhodium thin films and nanoparticles. The key steps and control methods of rhodium thin films and NPs synthesis were described in Part I (1). The effects of different shapes and sizes on various catalytic reactions provide a design basis for further industrial applications.

References

1. Y. Zhou, W. Wu, Q. Wang, L. Wang, *Johnson Matthey Technol. Rev*., 2024, **68**, (1), 91
2. S. Rai, U. Shaislamov, J. K. Yang, S. Saud, W. A. Muhammed, H. J. Lee, *J. Korean Phys. Soc.*, 2019, **75**, (8), 644
3. L. Marot, G. De Temmerman, P. Oelhafen, G. Covarel, A. Litnovsky, *Rev. Sci. Instrum.*, 2007, **78**, (10), 103507
4. A. T. T. Mostako, A. Khare, C. V. S. Rao, S. Vala, R. J. Makwana, T. K. Basu, *Nucl. Instrum. Meth. Phys. Res. Sect. B: Beam Interact. Mater. Atoms*, 2015, **342**, 150
5. J. Wrbanek, G. Fralick, S. Farmer, A. Sayir, C. Blaha, J. Gonzalez, 'Development of Thin Film Ceramic Thermocouples for High Temperature Environments', 40th AIAA/ASME/SAE/ASEE Joint Propulsion Conference and Exhibit, Fort Lauderdale, USA, 11th –14th July, 2004, No. AIAA 2004-3549, Institute of Aeronautics and Astronautics, Reston, USA, 2004
6. I. M. Tougas, M. Amani, O. J. Gregory, *Sensors*, 2013, **13**, (11), 15324
7. O. J. Gregory, T. You, *IEEE Sens. J.*, 2005, **5**, (5), 833
8. H. Choi, X. Li, *Sensors Actuators A: Phys.*, 2007, **136**, (1), 118
9. X. Zhao, H. Li, K. Yang, S. Jiang, H. Jiang, W. Zhang, *J. Alloys Compd.*, 2017, **698**, 147
10. A. Zribi, M. Barthès, S. Bégot, F. Lanzetta, J. Y. Rauch, V. Moutarlier, *Sensors Actuators A: Phys.*, 2016, **245**, 26
11. D. Liu, P. Shi, W. Ren, Y. Liu, G. Niu, M. Liu, N. Zhang, B. Tian, W. Jing, Z. Jiang, Z.-G. Ye, *J. Mater. Chem. C*, 2018, **6**, (13), 3206
12. Y. Liu, W. Ren, P. Shi, D. Liu, Y. Zhang, M. Liu, Z.-G. Ye, W. Jing, B. Tian, Z. Jiang, *Sensors*, 2018, **18**, (4), 958
13. Y. Liu, H. Jiang, X. Zhao, B. Liu, Z. Jia, X. Deng, W. Zhang, *Ceram. Int.*, 2022, **48**, (22), 33943
14. X. Jin, B. Ma, J. Deng, J. Luo, W. Yuan, *Ceram. Int*., 2021, **47**, 28411
15. Y. Wei, H. Liang, G. Wang, W. Xingqi, L. Yang, H. Zhou, L. Yang, X. Mu, G. Yin, *Ultrasonics*, 2021, **113**, 106361
16. Y. Wu, C. Luo, W. Wu, Q. Su, *J. Chem. Technol. Biotechnol.*, 2019, **94**, (9), 2969
17. M. Omrani, M. Goriaux, Y. Liu, S. Martinet, L. Jean-Soro, V. Ruban, *Environ. Pollut.*, 2020, **257**, 113477
18. Y. Lu, Z. Zhang, F. Lin, H. Wang, Y. Wang, *ChemNanoMat*, 2020, **6**, (12), 1659
19. L. Lan, S. Chen, S. Wang, J. Xiang, L. Huang, M. Zhu, H. Lin, *Arab. J. Chem.*, 2022, **15**, (2), 103587
20. B. Han, T. Li, J. Zhang, C. Zeng, H. Matsumoto, Y. Su, B. Qiao, T. Zhang, *Chem. Commun.*, 2020, **56**, (36), 4870
21. K. Ashida, H. Maeda, T. Araki, M. Hoshino, K. Hiraya, T. Izumi, M. Yasuoka, *SAE Int. J. Fuels Lubr.*, 2015, **8**, (2), 358
22. S. R. Gomes, N. Bion, G. Blanchard, S. Rousseau, V. Bellière-Baca, V. Harlé, D. Duprez, F. Epron, *Appl. Catal. B: Environ.*, 2011, **102**, (1–2), 44
23. M. Betchaku, Y. Nakagawa, M. Tamura, M. Yabushita, Y. Miura, S. Iida, K. Tomishige, *Fuel Process. Technol.*, 2022, **225**, 107061
24. X. Guo, Y. Wang, H. Zhang, D. Du, Z. Qi, *Environ. Prog. Sustain. Energy*, 2023, **42**, (4), e14073
25. W. Zang, G. Li, L. Wang, X. Zhang, *Catal. Sci. Technol*., 2015, **5**, (5), 2532
26. E. S. Vlasenko, I. A. Nikovskiy, Y. V Nelyubina, A. A. Korlyukov, V. V. Novikov, *Mendeleev Commun.*, 2022, **32**, (3), 320
27. S. García, L. Zhang, G. W. Piburn, G. Henkelman, S. M. Humphrey, *ACS Nano*, 2014, **8**, (11), 11512
28. T. Moriai, T. Tsukamoto, M. Tanabe, T. Kambe, K. Yamamoto, *Angew. Chem.*, 2020, **132**, (51), 23251
29. G. W. Piburn, H. Li, P. Kunal, G. Henkelman, S. M. Humphrey, *ChemCatChem*, 2018, **10**, (1), 329
30. L. Wang, Y. Li, M. Xia, Z. Li, Z. Chen, Z. Ma, X. Qin, G. Shao, *J. Power Sources*, 2017, **347**, 220
31. R. Niishiro, S. Tanaka, A. Kudo, *Appl. Catal. B: Environ.*, 2014, **150**–**151**, 187
32. S. Liu, M. Li, C. Wang, P. Jiang, L. Hu, Q. Chen, *ACS Sustain. Chem. Eng*., 2018, **6**, (7), 9137
33. J. Kim, H. Kim, S. H. Ahn, *ACS Sustain. Chem. Eng.*, 2019, **7**, (16), 14041
34. H. Guo, Z. Fang, H. Li, D. Fernandez, G. Henkelman, S. M. Humphrey, G. Yu, *ACS Nano*, 2019, **13**, (11), 13225
35. W. Shen, L. Ge, Y. Sun, F. Liao, L. Xu, Q. Dang, Z. Kang, M. Shao, *ACS Appl. Mater. Interfaces*, 2018, **10**, (39), 33153
36. X. Wu, R. Wang, W. Li, B. Feng, W. Hu, *ACS Appl. Nano Mater.*, 2021, **4**, (4), 3369
37. H. Duan, D. Li, Y. Tang, Y. He, S. Ji, R. Wang, H. Lv, P. P. Lopes, A. P. Paulikas, H. Li, S. X. Mao, C. Wang, N. M. Markovic, J. Li, V .R. Stamenkovic, Y. Li, *J. Am. Chem. Soc*., 2017, **139**, (15), 5494
38. L. Zhu, H. Lin, Y. Li, F. Liao, Y. Lifshitz, M. Sheng, S.-T. Lee, M. Shao, *Nat. Commun*., 2016, **7**, 12272
39. N.-F. Yu, N. Tian, Z.-Y. Zhou, L. Huang, J. Xiao, Y.-H. Wen, S.-G. Sun, *Angew. Chem. Int. Ed.*, 2014, **53**, (20), 5097
40. Y. Cheng, S. Lu, F. Liao, L. Liu, Y. Li, M. Shao,

Adv. Funct. Mater., 2017, **27**, (23), 1700359

41. A. M. Weisberg, *Metal Finish.*, 1999, **97**, (1), 297
42. B. Qu, X. Yu, Y. Chen, C. Zhu, C. Li, Z. Yin, X. Zhang, *ACS Appl. Mater. Interfaces*, 2015, **7**, (26), 14170
43. Y. Yin, Y. Zhang, T. Gao, T. Yao, X. Zhang, J. Han, X. Wang, Z. Zhang, P. Xu, P. Zhang, X. Cao, B. Song, S. Jin, *Adv. Mater.*, 2017, **29**, (28), 1700311
44. D. Gao, B. Xia, C. Zhu, Y. Du, P. Xi, D. Xue, J. Ding, J. Wang, *J. Mater. Chem. A*, 2018, **6**, (2), 510
45. Z. Zhu, X. Yang, J. Liu, M. Zhu, X. Xu, *Carbon Energy*, 2023, **5**, (10), e327
46. Z. Liu, N. Li, H. Zhao, Y. Du, *J. Mater. Chem. A*, 2015, **3**, (39), 19706
47. D. Gao, B. Xia, Y. Wang, W. Xiao, P. Xi, D. Xue, J. Ding, *Small*, 2018, **14**, (14), 1704150
48. L. Yu, B. Y. Xia, X. Wang, X. W. Lou, *Adv. Mater.*, 2016, **28**, (1), 92
49. X. Chen, Y. Qiu, G. Liu, W. Zheng, W. Feng, F. Gao, W. Cao, Y. Fu, W. Hu, P. Hu, *J. Mater. Chem. A*, 2017, **5**, (22), 11357

The Authors

Yicheng Zhou is a Master's research scholar under the guidance of Wangping Wu in the School of Mechanical Engineering and Rail Transit, Changzhou University, China. He received his BA from Suzhou University of Science and Technology, China, in 2020. His current research focuses on catalysis, energy, electrochemistry and corrosion. He has experience and knowledge in the preparation of thin films and nanoparticles by electrodeposition. He had the National scholarship for Postgraduates in 2023 and has published seven papers in peer-reviewed international journals and one patent.

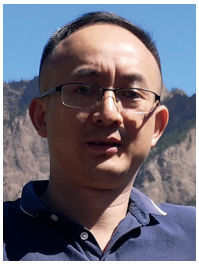

Wangping Wu received his PhD in Materials Processing Engineering from Nanjing University of Aeronautics and Astronautics, China, in 2013. He joined the Tel Aviv University, Israel, as a Postdoctoral Fellow from October 2013, and jointed the Hochschule Mittweida University of Applied Sciences, Germany, and Technische Universität Chemnitz, Germany, from September 2019 as a visiting scholar by the support of China Scholarship Council (CSC). He then joined the Engle Machinery Co, Ltd from January 2023 as a senior engineer. He currently works as an Associate Professor at the School of Mechanical Engineering and Rail Transit, Changzhou University, China. His research focuses on the synthesis, characterisation and performance of films and coatings of the noble metals and their alloys, nanopowders dispersed in polymer and electrochemical additive manufacturing. He has published over 100 papers in peer-reviewed international journals, over 10 invent patents and two books.

Qinqin Wang received her PhD in Materials Science and Engineering from Changzhou University, China, in 2022. She engaged in the photovoltaic industry for more than ten years and worked in LONGi Solar Technology Co, Ltd as a senior chief engineer. She currently works as a lecturer at the Institute of Technology for Carbon Neutralition, School of Mechanical Engineering, Yangzhou University, China. Her research focuses on the industrial application of high-efficiency crystalline silicon solar cell, structural design of tandem cell, optical and electrical matching and other issues. She has published over 20 papers in peer-reviewed international journals and over 10 invent patents.

Liangbing Wang is a Master's research scholar who graduated from the School of Materials Science and Technology, Nanjing University of Aeronautics and Astronautics. He is currently the executive deputy general manager of AVIC Surface Treatment Technology (Tianjin) Co, Ltd. He has been engaged in material heat treatment and surface treatment. He carries out basic research into type selection, heat treatment process, corrosion and protection of metal materials, process management, forward process design and process verification. He has published over 10 papers in peer-reviewed international journals and eight patents.